Niger. J. Physiol. Sci. 40 (June 2025): 179 – 190
www.njps.physiologicalsociety.com

Niger. J. Physiol. Sci.

Full-length Research Article

Therapeutic Effects of *Persea americana* L. Phytochemicals on Key Molecular Targets in Knee Osteoarthritis: *In-silico* and *In-vivo* approach

***Akintoye O.O.[1,2], Oniyide A.A.[2], Akintayo C.O.[3], Adeoluwa O.A.[4] and Olaniyi K.S.[2]**

[1.] *Neuro/Repro-Metabolic Unit, Physiology Department, College of Medicine, Department of Physiology, College of Medicine, Lead City University, Ibadan, Oyo State, Nigeria.*

[2.] *Cardio/Endo-metabolic and Epigenetic Research Unit, Department of Physiology, College of Medicine and Health Sciences, Afe Babalola University, Ado-Ekiti, 360101, Nigeria.*

[3] *Department of Medicine and Surgery, Faculty of Clinical Sciences, College of Health Sciences, Obafemi Awolowo University, Ile Ife, Nigeria.*

[4] *Department of Pharmacology and Therapeutics, College of Medicine and Health Sciences, Afe Babalola University, Ado-Ekiti, 360101, Nigeria*

Summary: Knee osteoarthritis (KOA) is a prevalent degenerative joint disorder characterized by chronic inflammation, cartilage degradation, and altered bone remodelling. This study investigated the inhibitory effects of *Persea americana* L. phytochemicals on key molecular targets involved in KOA pathogenesis and compared them with clinically used drugs targeting these pathways. Specifically, Interleukin receptor-associated kinase 4 (IRAK4), Transforming Growth Factor-Beta (TGF-β), Microsomal Prostaglandin E Synthase 1 (mPGES1), Kelch-like ECH-Associated Protein 1 (Keap1), Carbonic Anhydrase 1 (CA1), and Collagen II. Molecular docking analyses were performed using Schrodinger (Maestro 12.12). All proteins' 3D X-ray crystallographic structures were screened based on the following properties (Organism, Expression system, and Resolution) using the Protein Data Bank (RCSB PDB) https://www.rcsb.org/. Various lead compounds with significant binding affinities to these targets have been identified, outperforming conventional pharmacological agents. In vivo assessments using the hot plate test were conducted on 30 male Wistar rats, which were divided into six experimental groups. Chemical induction of KOA was performed by intra-articular injection of 25uL of saline dissolved 4 mg/kg of Sodium monoiodoacetate (MIA) in four of five groups: Control, Sham, and 3 treated with Ibuprofen, Low, and High *Persea americana* L. extracts, respectively, except the KOA only group. The docking scores from all the pathways showed higher binding energy when compared to the present drug samples, except for KEAP 1, where Chlorhexidine "STD" and Quercetin had binding scores of -6.576 and -6.557, respectively. *Persea americana* L. extracts treated rats showed significantly enhanced pain thresholds in KOA models compared to pathological untreated and ibuprofen-treated groups ($p<0.006$; 0.041 respectively) by Day 21 post-induction of KOA, indicating their analgesic efficacy. These results collectively highlight the potential of *Persea americana* L. phytochemicals as novel therapeutic agents for the management of knee osteoarthritis, with strong consideration of a systemic pharmacological approach.

Keywords*: Knee Osteoarthritis, Persea americana, Pain Modality Test, Molecular Docking, Pain threshold.*

**Authors for correspondence: olabode.akintoye@eksu.edu.ng, Tel: +234-7031830371*

Manuscript received- November 2024; Accepted: February 2025

DOI: https://doi.org/10.54548/njps.v40i1.X

INTRODUCTION

Osteoarthritis (OA) is the most common form of arthritis, affecting millions of individuals worldwide (Hawker 2019; Yao *et al*., 2023). The most common presentation is knee OA (KOA), which causes chronic knee pain, disability, and diminished quality of life in patients with KOA (Farrokhi *et al*., 2016; Vitaloni *et al*., 2019). Epidemiological data show that the global prevalence of knee OA is approximately 3.8% in men and 7.8% in women, of whom approximately 14 million adults are affected in the US (Chen *et al*., 2021; Allen *et al*., 2022). Knee OA pathogenesis involves an imbalance between catabolic and anabolic activity of the joint structures, including inflammation, redox imbalance, and apoptotic activities of the cartilage, bone, and synovium (Kapoor 2015; Primorac *et al*., 2020; Yunus *et al*., 2020). This has been identified as a potential target for therapeutic intervention and plays an important role in the disease process (Valenti *et al*., 2021).

IRAK4 is a vital mediator of the pathogenesis of knee osteoarthritis. Recently, it has played a central role in the Toll-like receptor (TLR) and interleukin 1 receptor (IL-1R) signaling pathways for proinflammatory responses (Li *et al*., 2021, Jrad *et al*., 2023). Activated interleukin-1 receptor-associated kinase 4 (IRAK4) promotes the production of proinflammatory cytokines, IL-1β and TNF-α, which induce cartilage matrix degradation (Jrad *et al*., 2023). Li *et al*., (2021) also reported that IRAK4 signalling disrupts chondrocyte function, inducing apoptosis and suppressing matrix synthesis. Furthermore, IRAK4 is implicated in bone remodeling, resulting in abnormal bone remodelling and osteophyte formation (Alonso-Perez *et al*., 2018). Likewise, Transforming Growth Factor-Beta (TGF-β) is a multifunctional cytokine with critical roles in the regulation of cellular processes, such as growth, differentiation, and extracellular matrix production (Tirado-Rodriguez *et al*., 2014). Elevated TGF-β levels in the subchondral bone are a major initiating factor in the pathogenesis of knee osteoarthritis (Macfarlane *et al*., 2017). However, increased TGF-β signalling is triggered by many factors, such as joint injury, mechanical stress, inflammation, genetic or epigenetic factors, metabolic disturbances, or ageing (Shen *et al*., 2017). Enhanced subchondral bone remodeling later in the process leads to the formation of new thicker sclerotic bone that is TGFβ-driven (Macfarlane *et al*., 2017). These alterations in the subchondral bone excessively change joint mechanics in the overlying articular cartilage and initiate a cascade of pathological remodeling in the cartilage, resulting in osteoarthritis.

The rate limiting step in the production pathway for bioactive PGE2 from Prostaglandin H2 (PGH2) is catalyzed by a single abundant form of microsomal Prostaglandin E Synthase 1 mPGES1 (Goodman 2018). mPGES1 increases the production of PGE2, a substance that promotes the development and progression of knee osteoarthritis. Jang *et al*., (2022) further reported that PGE2 is a potent proinflammatory mediator that leads to further cytokines and up regulation of osteoclast activity, leading to subchondral bone lesions. PGE2 also promotes synovial inflammation and angiogenesis and propagates osteoarthritis (Sanchez-Lopez *et al*., 2022). Kelch-like ECH-Associated Protein 1 (Keap1), a key regulator of the Nrf2 signaling pathway, is implicated in the pathogenesis of knee osteoarthritis (Khan *et al*., 2018). Oxidative stress and inflammation increase the induction of oxidative stress and inflammation disrupt the Keap1-Nrf2 interaction, leading Nrf2 to translocate to the nucleus and activate the expression of antioxidant and cytoprotective genes (Wen *et al*., 2019). However, dysregulation of the Keap1–Nrf2 axis is sustained and can alter chondrocyte function, leading to the progressive degeneration of articular cartilage (Riegger *et al*., 2023). However, these pathways result in collagen II depletion, breaking knee osteogenic homeostasis and causing cartilage breakdown, which is the hallmark of knee osteoarthritis (Gauci *et al*., 2017). Collagen II degradation is often initiated by an imbalance of enzymes, such as MMPs and aggrecanases, which can be upregulated by factors such as mechanical stress and joint inflammation pathogenesis (Mukherjee and Das 2024). Loss of the collagen II matrix results in knee cartilage thinning and erosion, exposing the underlying bones. This drives bone remodeling and osteophyte formation, further worsening the prognosis of knee osteoarthritis (Mukherjee and Das 2024).

With recent advancements in pharmaceutical technology, there has been an increasing awareness of the use of plant-based extracts in managing osteoarthritis (Yves *et al*., 2022), thus offering a promising alternative to conventional analgesics that are often clinically prescribed in this part of the world. This paradigm shift in the management approach can be based on the likely reduced burden of NSAID side effects and the multi-therapeutic window of the leaf extract, as they are rich in various bioactive compounds that provide additional therapeutic functions. Therefore, they can block multiple pathological pathways, such as inflammation, oxidative stress, anti-apoptotic, and chondroprotective pathways, simultaneously and not just alleviating pain alone (Silvia *et al*., 2018). *Persea americana*, commonly known as avocado, is a fruit-bearing tree native to central Mexico (Majid *et al*., 2020) that is readily found in Nigeria. Numerous studies have suggested that the fruit of *Persea americana* contains a variety of bioactive compounds, including polyphenols, flavonoids, and terpenoids, which exhibit potent anti-inflammatory, antioxidant, and chondroprotective properties (Sundararajan *et al*., 2023). These properties make *Persea americana* L. extract a promising candidate for managing knee osteoarthritis. The proposed study aims to investigate the role of *Persea americana* L. extract on experimental knee osteoarthritis using a multi-pronged approach involving in-silico molecular docking studies and in-vivo pain behavioral assessments.

MATERIALS AND METHODS

Phyto- Ligand Library creation: The chemical compounds were retrieved based on the chemical characterization of *Persea americana* L. reported by Wang *et al*. (2020) and Bonvehi *et al*. (2019). Ninety-nine (99) major compounds of *Persea americana* L. were retrieved using the search tool with the compound names, and the 2D structures of the phyto-ligands were retrieved from the PubChem Database (https://pubchem.ncbi.nlm.nih.gov) and saved in the Structure Data File (SDF) format.

Protein preparation and receptor grid generation: The 3D X-ray crystallographic structures of all proteins were retrieved from the Protein Data Bank (RCSB PDB). The protein receptor targets [TGF-B (PDB ID: 4UM8), mPGES-1 (PDB ID: 4YL3), KEAP1 (PDB ID: 5GIT), IRAK4 (PDB ID: 6EGF), Collagenase II (PDB ID: 6HG7), and CA-1 (5GMM)] were preprocessed, optimized, minimized, and refined using the Protein Preparation Wizard. During the prepossessing, bond orders and hydrogen bonds were assigned, and water molecules and other heteroatoms were removed during the pre-processing step, followed by energy minimization using the OPLS-3e force field available in Maestro 12.8. The active site x, y, and z coordinates of their respective centroid co-crystallized ligands were used to generate docking grid boxes saved in gridbox.zip files (Omoboyowa *et al*., 2021).

Protein-Ligand Docking: The Standard Precision (SP) was employed for the initial screening, and extra precision (XP) was used for the filtered ligands. Ligand docking was

performed using the Glide module of Schrodinger-Maestro v12. XP method was used to weed out false positives and provide a better correlation between good poses and good scores, estimate the theoretical interaction of the ligands with the proteins, and evaluate the interactions between the ligands and amino acids that were scored appropriately. Lower GlideScore signifies a Better Binding Affinity, which means that a more negative score means stronger predicted binding interaction (Schrödinger, 2020; Omoboyowa *et al*., 2021).

In-vivo Studies

Chemicals and Drugs: Sodium Monoiodoacetate was purchased from Santa Cruz Biotechnology (10410 Finnell Street, Dallas, USA). Ibuprofen was purchased from Aromokeye Pharmacy (Ado Ekiti, Nigeria). Phosphate buffer solution, Ethanol and Chloroform were obtained from the Department of Physiology Laboratory, College of Medicine, Ekiti State University, Ado Ekiti, Nigeria. Formalin was obtained from the Department of Anatomy, College of Medicine, Ekiti State University, Ado Ekiti, Nigeria.

SHK1 Extraction and Preparation of Sample (*Persea americana* L.): *Persea americana* leaves were obtained from a private farm in Ado Ekiti, botanically identified and authenticated at the Department of Plant Science, Ekiti State University, Ado- Ekiti with a herbarium voucher number UHAE2022071. Freshly collected leaves of *P. americana* were cleaned and dried in the shade at room temperature. After drying, the plant material was ground into smaller particles using a pestle and mortar and blended into a powder using an electric blender. The powdered sample (800 g) was then stored in airtight containers at room temperature until required. Extraction of *P. americana* L. was performed using 80% ethanol for 72 h. For extraction, the solvent was added 40 times the weight of the *P. americana* leaf powder. The extract was then filtered using a cheese cloth and freeze-dried. The supernatant from the dried extracts was then stored in airtight containers and kept at room temperature until required.

Experimental Animals: Thirty (30) wistar rats (180–220 g) were purchased from the breeding colony of the Department of Physiology, College of Medicine, Afe Babalola University, Ado Ekiti, Nigeria. The animals were maintained at 25°C on a 12hours light/dark cycle with access to food and water ad libitum. The animals were allowed to acclimatize under these conditions for two weeks before the commencement of the study and were kept under the same conditions throughout the study. This study was approved by the Ethics Review Committee of Afe Babalola University (protocol number: ABUADHREC/14/06/2024/466).

KOA induction model in Wistar rats: The infrapatellar ligament of the left knee (surgical point) was shaved after the animals were administered general anesthesia using a ketamine and xylazine combination (80/15 mg/kg body weight) administered intraperitoneally. The operation site was sterilized with chlorohexidine solution, after which a single intra-articular injection of 25uL of saline dissolved 4 mg/kg of sodium monoidoacetate (MIA), an inhibitor of aerobic glycolysis that directly injures the joint chondrocytes, was administered using a 17-gauge, 0.5 inch needle. The MIA dosage used followed that of Jiang *et al*. (2022), who reported the presentation of maximum joint discomfort at the specified dosage (Jiang *et al*., 2024).

Experimental Design: Thirty Male Wistar rats were randomly distributed into six groups (n = 5).
Group 1 (control group) received 1 ml/100 g body weight (b. w.) of water daily.
Group 2 (SHAM group) received 4 mg/kg dose of normal saline intra-articularly.
Groups 3-5 were induced with osteoarthritis (OA) by intra-articular injection of 4 mg/kg of sodium MIA in the right knee joint space. Animals in groups 3, 4, and 5 were treated for 18 days after KOA induction.
Group 3 (OA group) received intra-articular administration of 4 mg/kg of MIA.
Group 4 (OA+IBU group) received a 40 mg/kg b.w oral dose of ibuprofen.
Group 5 (OA + LDA group) received an oral dose of *P. americana* at a concentration of 50 mg/kg b.w. (Ogunmoyole *et al*., 2021)
Group 6 (OA + HDA group) received an oral dose of *P. americana* at a concentration of 100 mg/kg. (Ogunmoyole *et al*., 2021)

Measurement of Biometric Values of Pain threshold Test: All pain modality tests were performed weekly from day 0 until the last week of the experimental procedures using the hot plate test.

Hot Plate: This procedure was performed in accordance with the standard procedure described by Jimoh-Abdulghaffaar *et al*. (2023). Thermal hyperalgesia was assessed by placing animals on an electrical hot plate (maintained at 55°C ± 2 °C). The latency of the first sign of jumping off or paw licking by the animals from the hot plate was recorded in seconds by a blind observer as an index mark of pain threshold for that animal. A maximum time of 10 s was maintained for each procedure, after which the animal was immediately removed, regardless of whether the animal jumped. Pain response was measured at 30- and 60-minutes following extract administration. At no time was an animal allowed to stay on the hot plate for more than 10 seconds to avoid tissue damage.

Statistical Analysis: Data obtained from this study were analyzed using GraphPad Prism version 9.0 (GraphPad® Software, San Diego, CA, USA). Values are expressed as the mean ± SD. Groups were compared using one-way analysis of variance (ANOVA) followed by Tukey's post-hoc test for multiple comparisons to determine statistical significance.

RESULTS

Protein-Ligand Docking: The chemical structures of all the characterized phyto-compounds of *P. americana* are shown in Table 1.

Table 1
Chemical Structures from the Phytochemical Characterization of *Persea americana*

	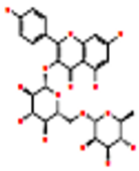	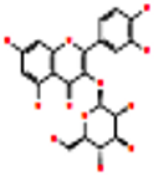	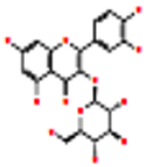	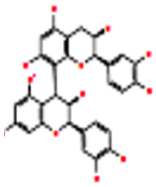
Title: 6EGF minimize	**Title:** 5318767	**Title:** 5280804	**Title:** 25203368	**Title:**
Entry name: 6EGF	**Entry name:** Nicotiflorin	**Entry name:** Isoquercitrin	**Entry name:** Quercetin	**Entry name:** epicathechin
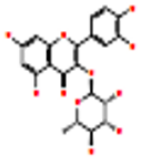	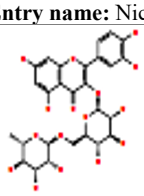	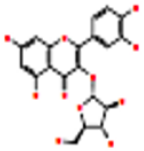	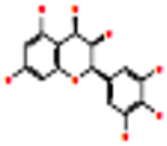	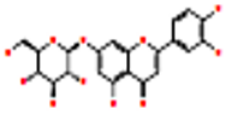
Title: 5280459	**Title:** 5280805	**Title:** 11968848	**Title:** 3081374	**Title:** 5280637
Entry name: quercitrin	**Entry name:** Rutin	**Entry name:** Quercetin-3-O	**Entry name:** Leukoefdin	**Entry name:** cynaroside
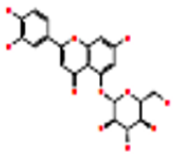	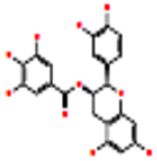	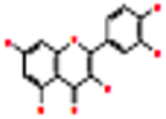	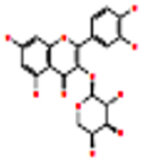	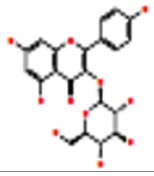
Title: 5317471	**Title:** 107905	**Title:** 5280343	**Title:** 44259270	**Title:** 5282102
Entry name: Luteolin 5-glucosi	**Entry name:** Epicatechin gallate	**Entry name:** quercetin	**Entry name:** quercetin3	**Entry name:** astragalin
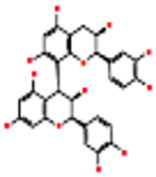	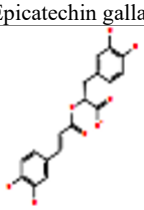	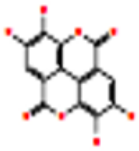	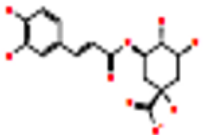	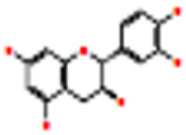
Title: 122738	**Title:** 5281792	**Title:** 5281855	**Title:** 1794427	**Title:** 9064
Entry name: epicathechin	**Entry name:** Rosmarinic acid	**Entry name:** Ellagic acid	**Entry name:** Chlorogenic acid	**Entry name:** cathechin
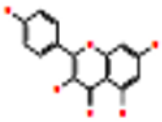	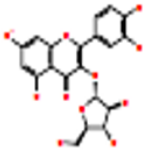	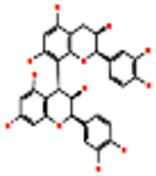	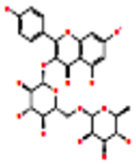	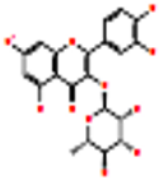
Title: 5280863	**Title:** 11968848	**Title:** 122738	**Title:** 5318767	**Title:** 5280459
Entry name: Kaempferol	**Entry name:** Quercetin-3-O-	**Entry name:** epicathechin	**Entry name:** Nicotiflorin	**Entry name:** quercitrin
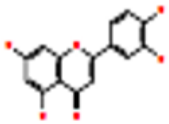	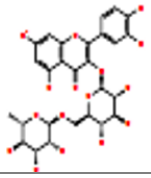	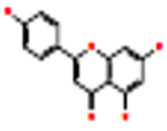	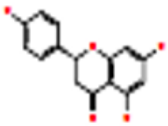	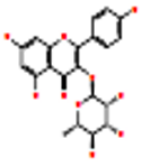
Title: 5280445	**Title:5280805**	**Title:5280443**	**Title:932**	**Title:** 5316673
Entry name luteolin	**Entry name** Rutin	**Entry name** apigenin	**Entry name** 5,7-Dihydroxy-	**Entry name:** Afzelin 1
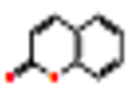	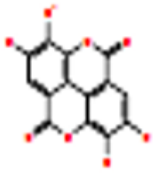	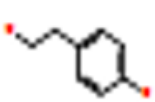	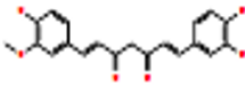	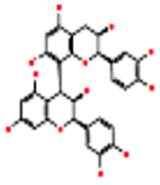
Title: 323	**Title:** 5281855	**Title:** 10393	**Title:** 969516	**Title:** 122738
Entry name: coumarin	**Entry name:** Ellagic acid.	**Entry name:** 2-(4-Hydroxyp	**Entry name:** Curcumin	**Entry name:** epicathechin

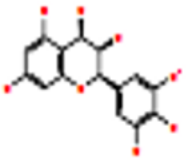	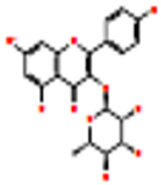	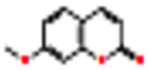	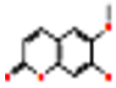	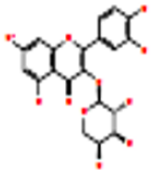
Title: 3081374	**Title:** 5316673	**Title:** 10748	**Title:** 5280460	**Title:** 5281855
Entry name: Leukoefdin	**Entry name:** afzelin	**Entry name:** 7-Methoxycou	**Entry name:** Scopoletin	**Entry name:** Elagic acid.1
	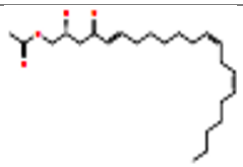		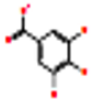	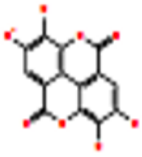
Title: 148675	**Title:** 9929676	**Title:** 9975455	**Title:** 370	**Title:** 5281855
Entry name: 3,4-Dihydroxy	**Entry name:** Persenone A.1	**Entry name:** Persenone B.1 .	**Entry name:** gallic acid.1	**Entry name:** Ellagic acid
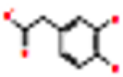	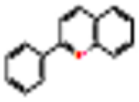	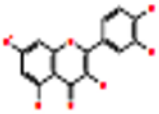	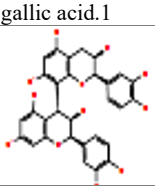	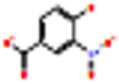
Title: 547	**Title:** 145858	**Title:** 5280343	**Title:** 122738	**Title:** 12033
Entry name:	**Entry name: anthocyanin**	**Entry name:** quercetin.	**Entry name:** epicathechin	**Entry name:** 4-hydroxybenz
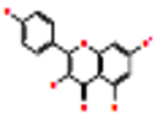		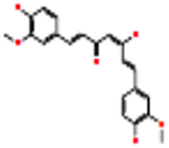	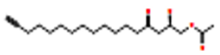	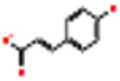
Title: 5280863	**Title:** 1057	**Title:** 969516	**Title:** 6710762	**Title:** 637542
Entry name: Kaempferol	**Entry name:** Pyrogallol	**Entry name:** Curcumin.	**Entry name:** 1-Acetoxy-2-h	**Entry name:** ecyn-4-one.1
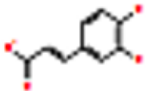	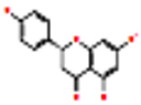		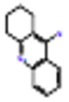	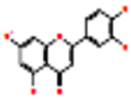
Title: 689043	**Title:** 932	**Title:** 107	**Title:** 1935	**Title:** 580445
Entry name: Caffeic acid.	**Entry name:** 5,7-Dihydroxy	**Entry name: hydrochroman-4-**	**Entry name: Tacrine**	**Entry name:** Luteolin.1
	4trihydrox 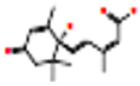	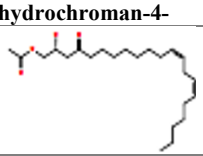		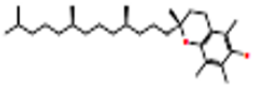
Title: 3015189	**Title:** 5375199	**Title:** 5283266	**Title:** 12021	**Title:** 14985
Entry name: Avocadyne	**Entry name:** Dormin	**Entry name:** Persin	**Entry name:** Dimethyl carbo	**Entry name:** tocopherol
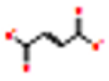	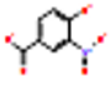	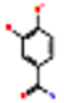	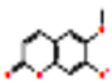	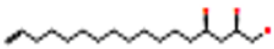
Title: 444972	**Title:** 12033	**Title:** 148675	**Title:** 5280460	**Title:** 21635755
Entry name: Fumaric acid.	**Entry name:** 4-hydroxybenz	**Entry name:** 3,4-Dihydroxy	**Entry name:** Scopoletin	**Entry name:** 1,2,4-Trihydro
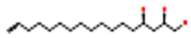	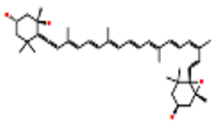	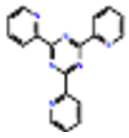	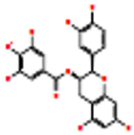	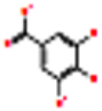
Title: 21635755	**Title:** 5282217	**Title:** 77258	**Title:** 107905	**Title:** 370
Entry name: 1,2,4trihydrox	**Entry name:** Neoxanthin	**Entry name:** 2,4,6-Tris(2-py	**Entry name:** Epicatechin gallate	**Entry name:** gallic acid

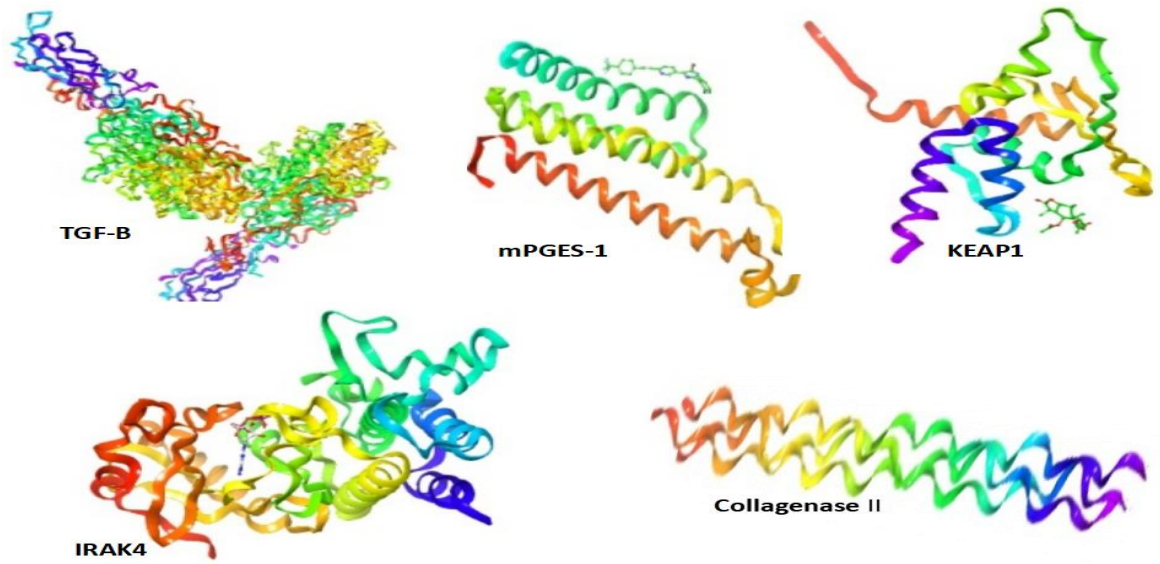

Figure 1:
X-ray Crystallography Structure of the Target Proteins: TGF-B (PDB ID: 4UM8), mPGES-1 (PDB ID: 4YL3), KEAP1 (PDB ID: 5GIT), IRAK4 (PDB ID: 6EGF), Collagenase II (PDB ID: 6HG7), CA-1 (5GMM)

The 2-dimensional structure of all the phyto-compounds present in *P. americana* in sdf format was docked against each of the active site of the target proteins: TGF-B (PDB ID: 4UM8), mPGES-1 (PDB ID: 4YL3), KEAP1 (PDB ID: 5GIT), IRAK4 (PDB ID: 6EGF), Collagenase II (PDB ID: 6HG7) and CA-1 (5GMM) (Fig. 1), along with the standard drugs Tranilast, Naproxen, Chlorhexidine, Zimlovisertib, Diclofenac, and TIMP1 (Tissue Inhibitor of Matrix Metalloproteinases 1) respectively. The docking results showed that 11 lead compounds exhibited good binding affinities with each of the target proteins (Fig. 2). Against the target protein TGF-B, all of the lead compounds have binding affinities ranging from -11.954Kcal/mol to -8.473Kcal/mol more than the standard drug Tranilast having binding affinity of -2.802Kcal/mol. Against mPGES-1, all the lead compounds exhibited good binding affinities, ranging from -6.787Kcal/mol to -5.158Kcal/mol, compared to the standard drug Naproxen, which had a binding affinity of -2.647Kcal/mol (Fig. 2). Against KEAP-1, the lead compounds exhibited good binding affinities ranging from -6.557Kcal/mol to -4.323Kcal/mol, and the standard drug Chlorhexidine exhibited a good binding affinity with a docking score of -6.576Kcal/mol. Against the target IRAK4, all the lead compounds exhibited good binding affinities ranging from -11.548Kcal/mol to -9.586 kcal/mol, better than the standard drug Zimlovisertib having binding affinity of -7.058Kcal/mol. Against the target Carbonic anhydrase 1, all the lead compounds exhibited good binding affinities with the target, with docking scores ranging from -6.385Kcal/mol to -4.749Kcal/mol, compared to the standard drug Diclofenac, which had a binding affinity of -1.967Kcal/mol. Against the target Collagenase II, nine of the lead compounds with docking scores ranging from -5.441Kcal/mol to -4.260Kcal/mol eahibited better binding affinities than the standard drug TIMP-1 with a binding affinity of -4.116Kcal/mol (Figure 2). The docking results showed that Quercetin 3-glucoside had the highest binding affinity against the target TGF-B than the standard drug Tranilast, Nicotiflorin had the highest binding affinity against the target IRAK4 compared to the standard drug Zimlovisertib, Quercetin 3-O-D-arabinopyranoside had the highest binding affinity against the target KEAP-1 and Collagenase II compared to the standard drugs Chlorhexidine and TIMP-1, respectively. Chlorogenic acid also had the highest binding affinity against the target mPGES-1 and Carbonic anhydrase 1 compared to the standard drugs Naproxen and Diclofenac, respectively (2).

Molecular Interactions: The 2-dimensional molecular interactions of the lead compounds with each of the standard drugs are illustrated in Figure 3. Figure 3a shows the 2D interaction of the compound Rutin, which has the highest binding affinity against the target TGF-B and the standard drug Tranilast. Figure 3b shows the 2D interaction of chlorogenic acid, which has the highest binding affinity against the target mPGES-1 and the standard drug Naproxen. Figure 3c shows the 2D interaction of the compound Quercetin 3-O-D-arabinopyranoside, which has the highest binding affinity among the lead compounds against the target KEAP-1 and the standard drug Chlorhexidine. The 2D interaction of the compound with the highest binding affinity for docking *P. americana* and Zimlovisertib against IRAK4 is depicted in Figure 3d. The 2D interaction of the highest-binding compound of The docking of the docking of *P. americana* Chlorogenic acid and the standard drug Diclofenac against the target Carbonic anhydrase 1 is shown in Figure 3e. Figure 3f shows the 2D interaction of Quercetin 3-O-D-arabinopyranoside, which has the highest binding affinity against the target Collagenase II and the standard drug TIMP1.

In-Silico Drug likeness, Pharmacokinetics, and Toxicity Prediction: The pharmacokinetics and toxicology predictions of all the lead compounds are depicted in Figure 4, showing hepatotoxicity, carcinogenicity, mutagenicity, immunotoxicity, Lipinski's rule of five, and other drug likeness predictions.

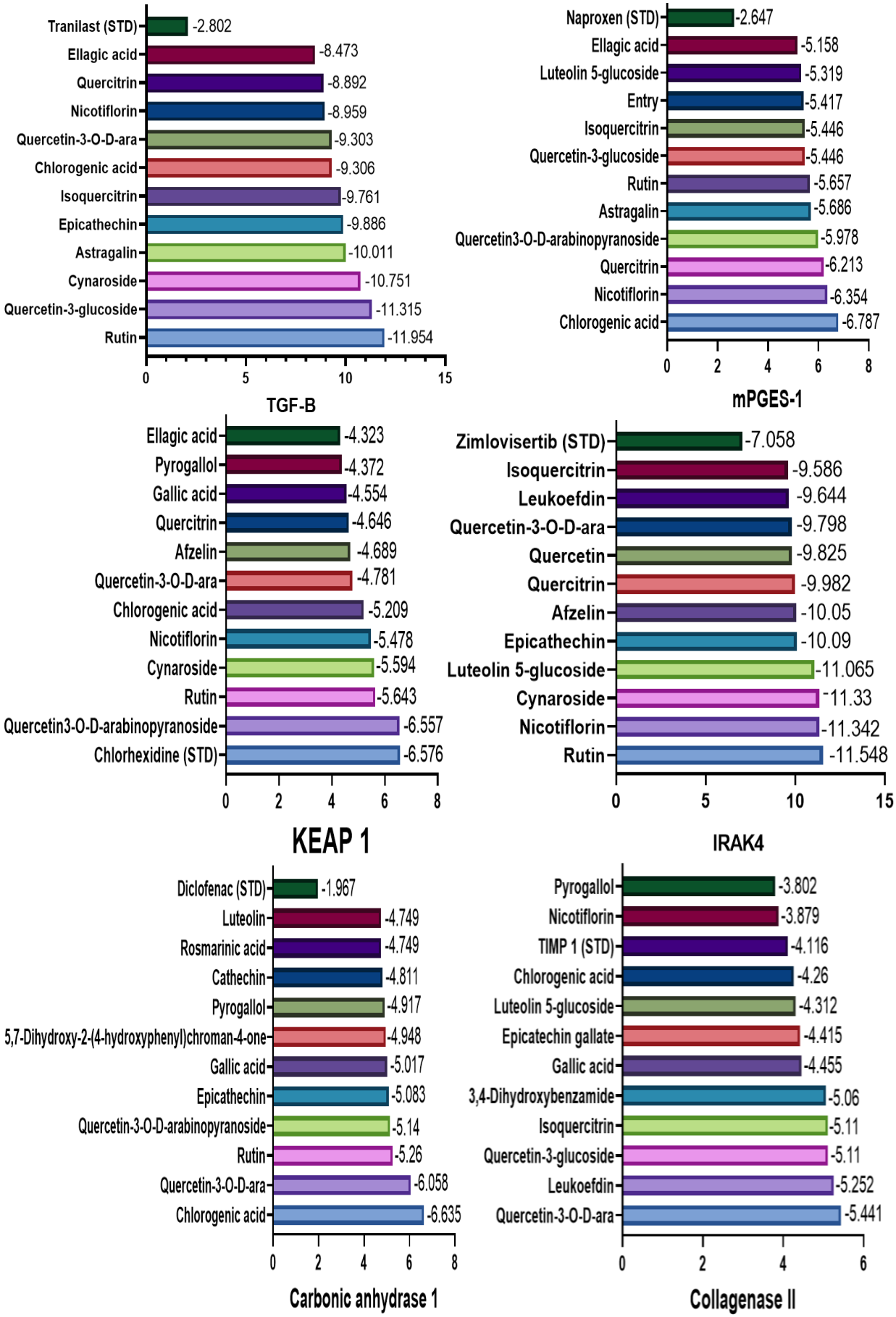

Figure 2:
Docking Scores/ Binding Affinities of the lead compounds from *Persea americana* docked against the target proteins

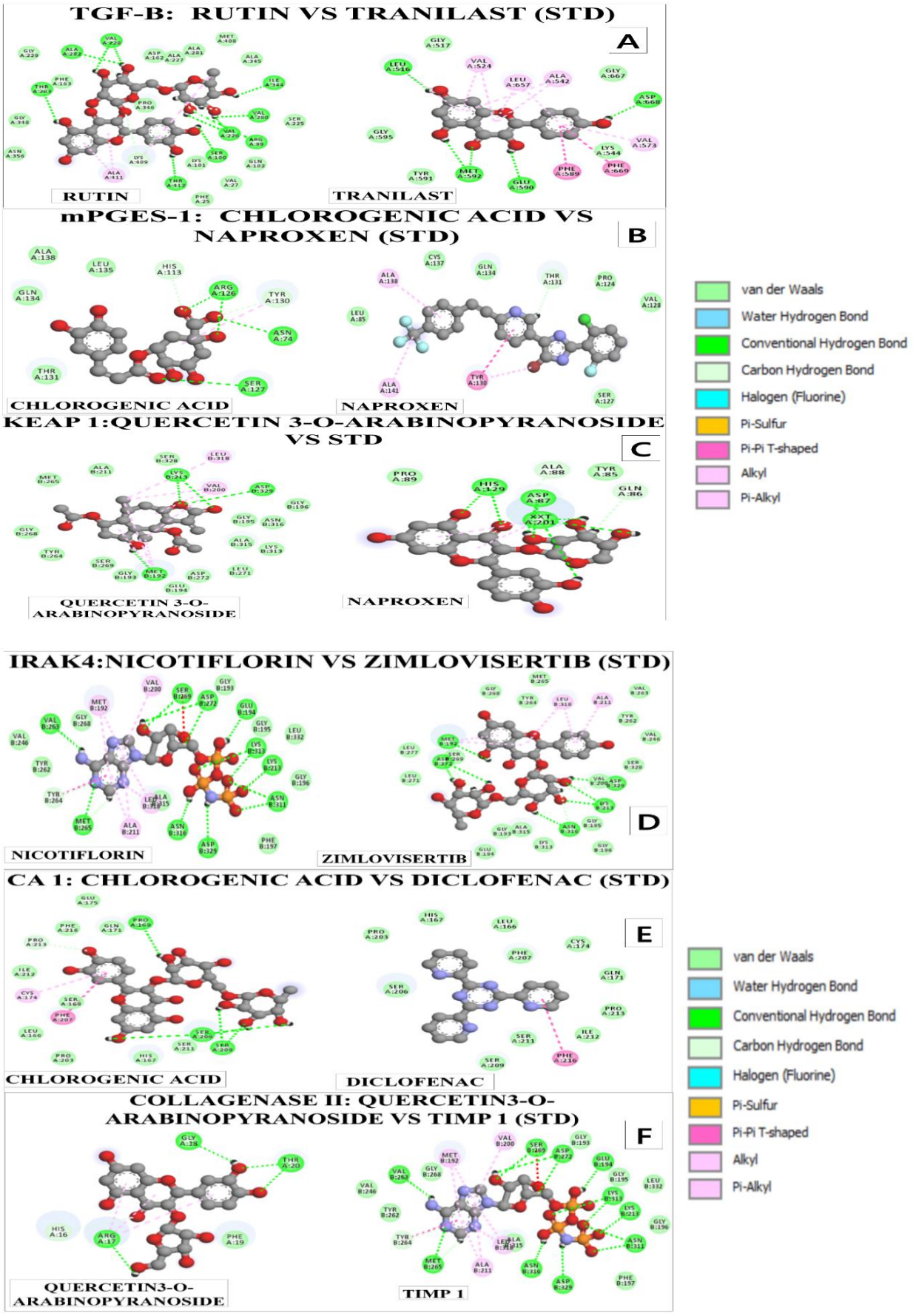

Figure 3:
2D-molecular interactions of the lead compounds from *Persea americana* docked against the target proteins.

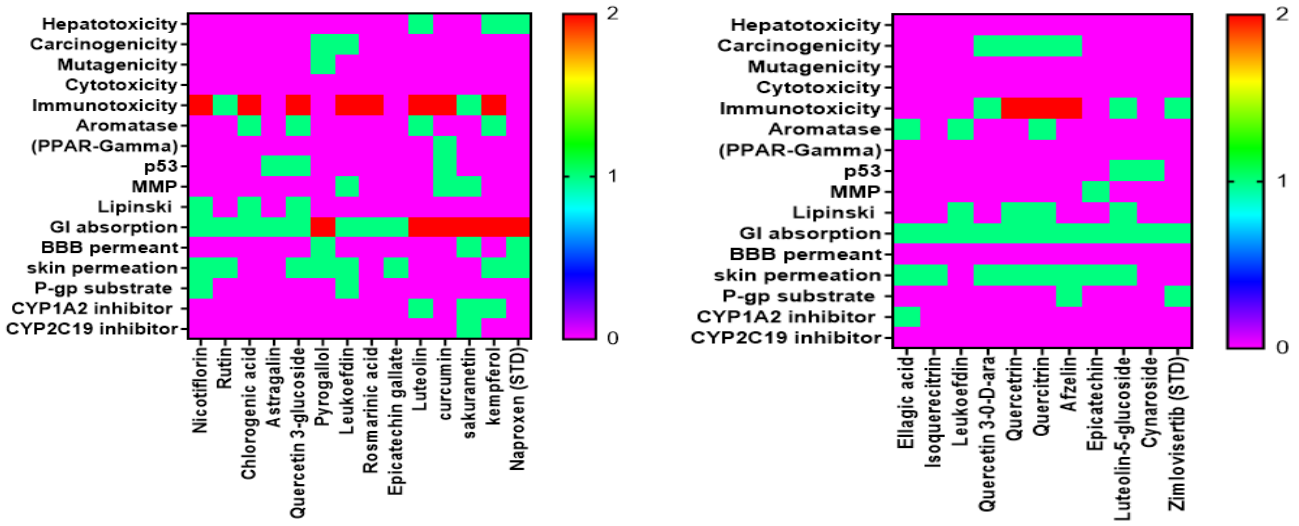

Figure 4:
Heat map showing the drug likeness and toxicity predictions of *Persea americana* lead compounds docked against the active site of all the target proteins

Table 2:
Effect of *Persea americana* L. dose-dependent treatment on the pain sensation threshold assessment of KOA-induced rats using the Hot Plate Test (s).

	CONTROL	SHAM	OA	OA+IBU	OA+LDA	OA+HDA
DAY 0	24.52±1.608	24.42±3.597	23.46±2.419	24.42±2.887	25.22±2.592	23.94±2.186
DAY 3	23.80±2.984	5.55±0.4924[a]	5.380±0.593[a]	5.320±1.370[a]	5.4±2.713[a]	5.540±3.024[a]
DAY 7	22.20±1.306	5.050±0.4528[a]	4.980±0.580[a]	6.140±1.737[a]	6±2.209[a]	6±2.014[a]
DAY 14	21.30±1.920	4.470±0.616[a]	4.1±0.741[a]	11.79±1.299[ab]	13.42±1.319[ab]	15.36±0.819[b]
DAY 21	20.36±0.650	4.170±0.426[a]	3.7±0.447[a]	15.19±0.959[ab]	16.62±1.416[b]	19.36±1.088[bc]

Control - 1 ml/100 g body weight (b. w.) of water daily; SHAM group received 4 mg/kg dose of normal saline; OA group received 4 mg/kg of MIA; OA+IBU group received 40 mg/kg b.w oral dose of ibuprofen; OA + LDA group received 50 mg/kg b.w of *P. americana* p.o; OA + HDA group received received 100 mg/kg b.w of *P. americana* p.o

Pain Modality Test

Effect of *Persea americana* L. Extract on Hot plate Test: The results of the pain threshold using the Hot Plate test across the six groups are shown in Table 2. The baseline measurement on day 0 showed no significant differences across the six groups. On day 3 (post-induction), our results showed a significantly decreased pain threshold in groups 2-6, relative to the control group. On day 7 post-treatment, all treatment groups showed statistically lower pain thresholds compared with the control group (p=0.0041; 0.0113; 0.0005; 0.0141), and by day 21 post-treatment, our results showed an improvement in the pain response sensitivity, with the OA+HDA treatment group demonstrating more potent amelioration of the pain response compared to the OA and OA+IBU groups (p=0.0012; 0.0417, respectively).

Table 2 shows the effect of *Persea americana* L. dose-dependent treatment on the pain sensation threshold assessment of a KOA induced rat by the hot plate test (secs) expressed as mean±SD, n =5. Data were analysed by one-way ANOVA followed by Tukey's multiple post hoc test. ap < 0.05 vs. Control, bp < 0.05 vs. OA cp < 0.05 vs. OA+IBU. OA (Osteoarthritis), IBU (Ibuprofen), LDA (Low dose *Persea americana* L.), HDA (High dose *Persea americana* L.).

DISCUSSION

Knee osteoarthritis is characterized by a complex interplay between inflammatory processes, cartilage degeneration, and altered bone remodeling (De Roover *et al*., 2023). The disease involves an imbalance between catabolic and anabolic activities within the joint, primarily driven by dysregulation of cytokines and other signaling molecules (Yunus *et al*., 2020). Key proteins such as Interleukin receptor-associated kinase 4 (IRAK4), Transforming Growth Factor-Beta (TGF-β), Microsomal Prostaglandin E Synthase 1 (mPGES1), Kelch-like ECH-Associated Protein 1 (Keap1), Carbonic Anhydrase 1 (CA1), and Collagen II play critical roles in these processes. Targeting these proteins may be an attractive strategy to limit KOA progression. Molecular docking studies showed that all lead compounds from *Persea americana* L. showed favorable binding affinities against the target proteins, which were significantly better than those of the standard drugs. The values were well above the binding affinity of the standard

drug, Tranilast, which was measured at -2.802 kcal/mol. [SHK1] The high binding affinities observed likely make these phyto compounds powerful inhibitors of TGF β activity, a key mediator of inflammatory responses and fibrotic pathologies in KOA (Zhang *et al*., 2021). Interactions between the lead compounds and TGF-β suggest the ability of these compounds to modulate the signaling pathways that promote cartilage degradation and joint inflammation by binding to this protein target, thus preventing its activation effect in KOA pathogenesis. The docking results for mPGES-1 showed a total binding affinity for the compounds ranging from -6.787 kcal/mol to -5.158 kcal/mol. The standard drug Naproxen bound to this site with a binding affinity of -2.647 kcal/mol. The high binding affinities of the lead compounds suggest that they may be good inhibitors of mPGES-1, an enzyme that is the chief prostaglandin E2 (a key mediator of pain and inflammation) synthesizing enzyme (Dos Santos Nascimento *et al*., 2022). The inhibition of these compounds could potentially reduce the inflammatory response of KOA, leading to therapeutic pain relief and joint function improvement. The lead compounds exhibited excellent binding affinities in the range of -6.557 to -4.323 kcal/mol in the docking study of Keap1. The comparable binding affinity observed for our standard drug, Chlorhexidine, was -6.576 kcal/mol. Thus, the results of this study indicate that phyto-compounds can efficiently fine-tune the Keap1-Nrf2 signaling module and regulate cellular antioxidant defenses as well as inflammatory states (Tu *et al*., 2019). By enhancing the activation of Nrf2, these compounds could contribute to the mitigation of oxidative stress in the joints, further supporting their potential role in the management of KOA.

The docking results for IRAK4 indicated that the lead compounds exhibited binding affinities that were significantly higher than that of Zimlovisertib, a standard drug used to block this pathway in clinical practice. The affinities for these compounds are sufficiently strong to suggest that they can effectively inhibit IRAK4, a key kinase in the inflammatory signaling cascade. Thus, the combination of these compounds with IRAK4 targeting might reduce the inflammatory responses involved in the progression of KOA and present a novel therapeutic approach (Deligiannidou *et al*., 2020). For CA1, the binding affinities of the lead compounds ranged from -6.385 to -4.749 kcal/mol. The standard drug Diclofenac showed a much lower binding affinity of -1.967 kcal/mol. The findings suggest that the phyto-compounds may inhibit CA1, an enzyme that helps regulate pH and bicarbonate levels in the tissues. Inhibiting both PDR mice and KOA, these compounds could modulate the inflammatory processes within each joint; subsequently, these compounds may also influence the metabolic environment of the cartilage and synovial fluid in KOA (Wang *et al*., 2022). The docking results for Collagenase II showed that nine of the lead compounds exhibited binding affinities ranging from -5.441 kcal/mol to -4.260 kcal/mol. The standard drug TIMP-1 had a binding affinity of -4.116 kcal/mol. These findings indicate that phyto compounds prevent collagenase activity from degrading collagen in cartilage (Mixon *et al*., 2022). These compounds would prevent (or slow) the progression of KOA by inhibiting collagenase, which is one of the critical aspects of KOA progression; thus, this could potentially help preserve cartilage integrity and function.

Drug likeness and toxicity predictions of various lead molecules (from *Persea americana* L.) were analyzed in a heat map to provide insight into their potential as therapeutic agents for knee osteoarthritis (KOA). Lipinski's Rule of Five (Chen *et al*., 2020) was applied to each compound to rank the key drug-like properties of the compounds. The profiles of these compounds, such as Nicotiflorin, Quercetin 3-glucoside, and Chlorogenic Acid, all with favorable profiles, suggest their possible oral bioavailability and systemic absorption. The heat map also shows the toxicity of the lead compounds in terms of hepatotoxicity, carcinogenicity, and mutagenicity. Of particular note are Nicotiflorin and Quercetin 3-glucoside, which demonstrated lower toxicity predictions and are therefore good candidates for further development. Conversely, compounds such as Leukoefidin and its derivatives have higher toxicity risks, which may limit their clinical usefulness. Additionally, the assessment of gastrointestinal absorption and blood-brain barrier permeability revealed that several lead compounds, including Chlorogenic Acid, may not only alleviate pain associated with KOA but also have the potential for central nervous system effects, enhancing their therapeutic efficacy. Comparing these natural compounds with established drugs, such as Naproxen, provides a benchmark for evaluating their safety and efficacy. The heat map indicates that some lead compounds align closely with conventional therapies, suggesting that they could serve as effective alternatives or adjuncts in KOA treatment.

The analgesic property of *Persea americana* L.extracts was further evaluated by using standard Hot plate rat model test for measurement of nociceptive responses (Bannon and Malmberg, 2007; Oyesanmi *et al*.,2019). According to our results at different stages of pain assessment, as shown in Table 3.5.1, the group treated with the high dose of the extract demonstrated the best analgesic control compared to all other treatment groups. It is evident that this analgesic potential of *Persea americana* L extract is due to its multiple modulating effects on inflammation pathways and its strong supportive effect on collagen matrix integrity in KOA, as shown in the *in silico* segment of the study. Therefore, the *in vivo* pain behavioral assessments underscore the substantial analgesic effects of *Persea americana* L. extracts, further affirming its potential as an alternative therapeutic option for managing pain in knee osteoarthritis. As shown in this study, the sustained improvements in pain thresholds over the study period are further supported by our *in silico* results, which underline that natural compounds of *Persea americana* L. are efficacious for the management of chronic pain, thus motivating further investigation into their mechanisms and possible clinical applications in the management of chronic pain.

Together with in silico and in vivo validation, this study highlights the promising therapeutic potential of *Persea americana* L. compounds as inhibitors of key inflammatory and cartilage-degrading proteins in knee osteoarthritis. Our molecular docking results indicate that these phyto-compounds have higher binding affinities than currently used pharmacological agents being clinically utilized in the management of chronic pain, particularly against TGF-β and IRAK4, which are important in inflammatory mechanisms pertinent to KOA.

REFERENCES

Allen, K. D., Thoma, L. M., & Golightly, Y. M. (2022). Epidemiology of osteoarthritis. *Osteoarthritis and cartilage*, 30(2), 184-195.

Alonso-Pérez, A., Franco-Trepat, E., Guillán-Fresco, M., Jorge-Mora, A., López, V., Pino, J., & Gómez, R. (2018). Role of toll-like receptor 4 on osteoblast metabolism and function. *Frontiers in physiology*, 9, 504.

Arendt-Nielsen, L. (2017). Pain sensitisation in osteoarthritis. *Clin Exp Rheumatol*, 35(Suppl 107), 68-74.

Bannon, A. W., & Malmberg, A. B. (2007). Models of nociception: hot-plate, tail-flick, and formalin tests in rodents. *Current protocols in neuroscience*, 41(1), 8-9.

Bonvehi, J. S., Coll, F. V., & Bermejo, J. O. (2019). Characterization of avocado honey (*Persea americana* Mill.) produced in Southern Spain. *Food chemistry*, 287, 214-221.

Chen, H., Wu, J., Wang, Z., Wu, Y., Wu, T., Wu, Y., ... & Shang, S. (2021). Trends and patterns of knee osteoarthritis in China: a longitudinal study of 17.7 million adults from 2008 to 2017. *International Journal of Environmental Research and Public Health*, 18(16), 8864.

Chen, X., Li, H., Tian, L., Li, Q., Luo, J., & Zhang, Y. (2020). Analysis of the physicochemical properties of acaricides based on Lipinski's rule of five. *Journal of computational biology*, 27(9), 1397-1406.

De Roover, A., Escribano-Núñez, A., Monteagudo, S., & Lories, R. (2023). Fundamentals of osteoarthritis: Inflammatory mediators in osteoarthritis. *Osteoarthritis and Cartilage*, 31(10), 1303-1311.

Deligiannidou, G. E., Papadopoulos, R. E., Kontogiorgis, C., Detsi, A., Bezirtzoglou, E., & Constantinides, T. (2020). Unraveling natural products' role in osteoarthritis management—An overview. *Antioxidants*, 9(4), 348.

Dos Santos Nascimento, I. J., de Aquino, T. M., & da Silva Júnior, E. F. (2022). Computer-aided drug design of anti-inflammatory agents targeting microsomal prostaglandin E2 synthase-1 (mPGES-1). *Current medicinal chemistry*, 29(33), 5397-5419.

Farrokhi, S., Chen, Y. F., Piva, S. R., Fitzgerald, G. K., Jeong, J. H., & Kwoh, C. K. (2016). The influence of knee pain location on symptoms, functional status, and knee-related quality of life in older adults with chronic knee pain: data from the osteoarthritis initiative. *The Clinical journal of pain*, 32(6), 463-470.

Gauci, S. J., Stanton, H., Little, C. B., & Fosang, A. J. (2017). Proteoglycan and collagen degradation in osteoarthritis. Cartilage: Volume 2: *Pathophysiology*, 41-61.

Goodman, M. C. (2018). Investigations of the enzymatic mechanisms and inhibition of prostaglandin E2 biosynthesis. Vanderbilt University

Hawker, G. A. (2019). Osteoarthritis is a serious disease. Clin Exp Rheumatol, 37(Suppl 120), 3-6.

Jiang, W., Jin, Y., Zhang, S., Ding, Y., Huo, K., Yang, J., ... & Luo, J. (2022). PGE2 activates EP4 in subchondral bone osteoclasts to regulate osteoarthritis. *Bone research*, 10(1), 27.

Jiang, X., Guo, Y., Fang, M., Wang, X., Zhang, B., Song, Y., & Qian, J. (2024). Suppression of CGRP and TRPV1 Expression in Dorsal Root Ganglia of Knee Osteoarthritis Rats by Huojing Decoction via TrkA/MKK3/6/p38 Pathway. *Journal of Inflammation Research*, 5311-5326.

Jimoh-Abdulghaffaar HO, Ajibare AJ, Akintoye OO, Jimoh OS, Ananias EN, Owoyemi JO, Ibiyeye VO, Ojulari LS. Ficus exasperata leaves aqueous extract influences pathophysiolgic mechanisms of diabetic peripheral neuropathy in a rat model. *J Appl Pharm Sci*; 13(09):077–083 (2023). DOI: 10.7324/JAPS.2023.98174

Jrad, A. I. S., Trad, M., Bzeih, W., El Hasbani, G., & Uthman, I. (2023). Role of pro-inflammatory interleukins in osteoarthritis: a narrative review. *Connective Tissue Research*, 64(3), 238-247.

Kapoor, M. (2015). Pathogenesis of osteoarthritis. Osteoarthritis: pathogenesis, diagnosis, available treatments, drug safety, regenerative and precision medicine, 1-28.

Khan, N. M., Ahmad, I., & Haqqi, T. M. (2018). Nrf2/ARE pathway attenuates oxidative and apoptotic response in human osteoarthritis chondrocytes by activating ERK1/2/ELK1-P70S6K-P90RSK signaling axis. *Free Radical Biology and Medicine*, 116, 159-171.

Li, M., Li, H., Ran, X., Yin, H., Luo, X., & Chen, Z. (2021). Effects of adenovirus-mediated knockdown of IRAK4 on synovitis in the osteoarthritis rabbit model. *Arthritis Research & Therapy*, 23, 1-12.

MacFarlane, E. G., Haupt, J., Dietz, H. C., & Shore, E. M. (2017). TGF-β family signaling in connective tissue and skeletal diseases. Cold Spring Harbor perspectives in biology, 9(11), a022269.

Majid, D., Dar, B. N., Parveen, S., Jabeen, A., Allai, F. M., Sofi, S. A., & Ganaie, T. A. (2020). Avocado. Antioxidants in Fruits: *Properties and Health Benefits*, 103-123.

Mixon, A., Bahar-Moni, A. S., & Faisal, T. R. (2022). Mechanical characterization of articular cartilage degraded combinedly with MMP-1 and MMP-9. Journal of the mechanical behavior of biomedical materials, 129, 105131.

Mukherjee, A., & Das, B. (2024). The role of inflammatory mediators and matrix metalloproteinases (MMPs) in the progression of osteoarthritis. *Biomaterials and Biosystems*, 100090.

Omoboyowa DA, Karigidi KO, Aribigbola TC (2021) Nephro-protective efficacy of Blighia sapida s bark ether fractions on experimentally induced diabetes nephropathy. Comp Clin Pathol. https://doi.org/10.1007/s00580-020-03186-w.

Temidayo Ogunmoyole, Iretiogo Dada and Oluwatosin Adebukola Adebamigbe (2021) Ameliorative potentials of *Persea americana* leaf extract on toxicants - induced oxidative assault in multiple organs of wistar albino rat *Clinical Phytoscience* 7:27 https://doi.org/10.1186/s40816-020-00237-1

Oyesanmi Abisoye Fabunmi, Olabode Oluwadare Akintoye, Olutayo Folajimi Olaseinde, Ayonbo Adeolu Aderibigbe, Bamidele Victor Owoyele (2019). Anti-nociceptive effect of glycyrrhiza glabra root extract on chronic constriction injury of sciatic nerve induced neuropathic pain and some selected inflammatory biomarkers in experimental animals. Pacific *Journal of Medical Sciences*, Vol. 19(2); 13-22. ISSN: 2072 – 1625.

Primorac, D., Molnar, V., Rod, E., Jeleč, Ž., Čukelj, F., Matišić, V., ... & Borić, I. (2020). Knee osteoarthritis: a review of pathogenesis and state-of-the-art non-operative therapeutic considerations. *Genes*, 11(8), 854.

Riegger, J., Schoppa, A., Ruths, L., Haffner-Luntzer, M., & Ignatius, A. (2023). Oxidative stress as a key modulator of cell fate decision in osteoarthritis and osteoporosis: a narrative review. *Cellular & molecular biology letters*, 28(1), 76.

Sanchez-Lopez, E., Coras, R., Torres, A., Lane, N. E., & Guma, M. (2022). Synovial inflammation in osteoarthritis progression. *Nature Reviews Rheumatology*, 18(5), 258-275.

Schrödinger, LLC, Glide, 2020. Available at: https://www.schrodinger.com/glide.

Shen, J., Abu-Amer, Y., O'keefe, R. J., & McAlinden, A. (2017). Inflammation and epigenetic regulation in osteoarthritis. *Connective tissue research*, 58(1), 49-63.

Silvia Ravalli, Marta Anna Szychlinska, Rosalia Maria Leonardi, Giuseppe Musumeci. (2018) Recently highlighted nutraceuticals for preventive management of osteoarthritis. *World J Orthop* 2018 November 18; 9(11): 255-261. DOI: 10.5312/wjo.v9.i11.255

Sundararajan, N., Solomon, W. S., Jeevanandham, S., Ranganathan, K., Divakar, M. C., & Senthilkumar C (2023). in vitro and in vivo anti-alzheimer's activities of ethanolic leaf extract of *Persea americana* mill on scopolamine induced dementia in rat models. *Eur. Chem. Bull*. 12(Issue 7), 2214-2221

Tirado-Rodriguez, B., Ortega, E., Segura-Medina, P., & Huerta-Yepez, S. (2014). TGF-β: An Important Mediator of Allergic Disease and a Molecule with Dual Activity in Cancer Development. *Journal of immunology research*, 2014(1), 318481.

Tu, W., Wang, H., Li, S., Liu, Q., & Sha, H. (2019). The anti-inflammatory and anti-oxidant mechanisms of the Keap1/Nrf2/ARE signaling pathway in chronic diseases. *Aging and disease*, 10(3), 637.

Valenti, M. T., Dalle Carbonare, L., Zipeto, D., & Mottes, M. (2021). Control of the autophagy pathway in osteoarthritis: key regulators, therapeutic targets and therapeutic strategies. *International Journal of Molecular Sciences*, 22(5), 2700.

Vitaloni, M., Botto-van Bemden, A., Sciortino Contreras, R. M., Scotton, D., Bibas, M., Quintero, M., ... & Verges, J. (2019). Global management of patients with knee osteoarthritis begins with quality of life assessment: a systematic review. *BMC musculoskeletal disorders*, 20, 1-12.

Wang, M., Yu, P., Chittiboyina, A. G., Chen, D., Zhao, J., Avula, B., ... & Khan, I. A. (2020). Characterization, quantification and quality assessment of avocado (*Persea americana* Mill.) oils. *Molecules*, 25(6), 1453.

Wang, Z., Efferth, T., Hua, X., & Zhang, X. A. (2022). Medicinal plants and their secondary metabolites in alleviating knee osteoarthritis: A systematic review. *Phytomedicine*, 105, 154347.

Wen, Z., Liu, W., Li, X., Chen, W., Liu, Z., Wen, J., & Liu, Z. (2019). A protective role of the NRF2-Keap1 pathway in maintaining intestinal barrier function. *Oxidative medicine and cellular longevity,* 2019(1), 1759149.

Yao, Q., Wu, X., Tao, C., Gong, W., Chen, M., Qu, M., ... & Xiao, G. (2023). Osteoarthritis: pathogenic signaling pathways and therapeutic targets. *Signal transduction and targeted therapy*, 8(1), 56.

Yunus, M. H. M., Nordin, A., & Kamal, H. (2020). Pathophysiological perspective of osteoarthritis. *Medicina*, 56(11), 614.

Yunus, M. H. M., Nordin, A., & Kamal, H. (2020). Pathophysiological perspective of osteoarthritis. *Medicina*, 56(11), 614.

Yves Henrotin, Romain Le Cozannet , Pascale Fança Berthon, Romain Truillet, Martine Cohen Solhal, Gillian DunnGalvin, Jean Marie Grouin and Andrea Doolan. (2022) Rubus idaeus extract improves symptoms in knee osteoarthritis patients: results from a phase II double-blind randomized controlled trial. *BMC Musculoskeletal Disorders.* 23:650 https://doi.org/10.1186/s12891-022-05612-2

Zhang, L., Li, X., Zhang, H., Huang, Z., Zhang, N., Zhang, L., ... & Wang, P. (2021). Agnuside Alleviates Synovitis and Fibrosis in Knee Osteoarthritis through the Inhibition of HIF-1α and NLRP3 Inflammasome. *Mediators of Inflammation*, 2021(1), 5534614..